Journal of Biomedical Optics

SPIEDigitalLibrary.org/jbo

Photopolymerizable hydrogels for implants: Monte-Carlo modeling and experimental *in vitro* validation

Andreas Schmocker
Azadeh Khoushabi
Constantin Schizas
Pierre-Etienne Bourban
Dominique P. Pioletti
Christophe Moser

SPIE

Photopolymerizable hydrogels for implants: Monte-Carlo modeling and experimental *in vitro* validation

Andreas Schmocker,[a,b,*] Azadeh Khoushabi,[b,c] Constantin Schizas,[d] Pierre-Etienne Bourban,[c] Dominique P. Pioletti,[b] and Christophe Moser[a]
[a]Swiss Federal Institute of Technology Lausanne, Microengineering Institute, Laboratory of Applied Photonics Devices, station 17, Lausanne 1015, Switzerland
[b]Swiss Federal Institute of Technology Lausanne, Institute of Bioengineering, Laboratory of Biomechanical Orthopedics, station 19, Lausanne 1015, Switzerland
[c]Swiss Federal Institute of Technology Lausanne, Institute of Materials, Laboratory of Polymer and Composite Technology, station 12, Lausanne 1015, Switzerland
[d]Centre Hospitalier Universitaire Vaudois, Orthopedic Department, Avenue P. Decker 4, Lausanne 1011, Switzerland

Abstract. Photopolymerization is commonly used in a broad range of bioapplications, such as drug delivery, tissue engineering, and surgical implants, where liquid materials are injected and then hardened by means of illumination to create a solid polymer network. However, photopolymerization using a probe, e.g., needle guiding both the liquid and the curing illumination, has not been thoroughly investigated. We present a Monte Carlo model that takes into account the dynamic absorption and scattering parameters as well as solid–liquid boundaries of the photopolymer to yield the shape and volume of minimally invasively injected, photopolymerized hydrogels. In the first part of the article, our model is validated using a set of well-known poly(ethylene glycol) dimethacrylate hydrogels showing an excellent agreement between simulated and experimental volume-growth-rates. In the second part, *in situ* experimental results and simulations for photopolymerization in tissue cavities are presented. It was found that a cavity with a volume of 152 mm^3 can be photopolymerized from the output of a 0.28-mm^2 fiber by adding scattering lipid particles while only a volume of 38 mm^3 (25%) was achieved without particles. The proposed model provides a simple and robust method to solve complex photopolymerization problems, where the dimension of the light source is much smaller than the volume of the photopolymerizable hydrogel. [DOI: 10.1117/1.JBO.19.3.035004]

Keywords: photopolymerization; hydrogel; Monte Carlo; poly(ethylene glycol) dimethacrylate; fiber probe; scattering additive; simulation and modeling; intervertebral disc.

Paper 130811R received Nov. 13, 2013; revised manuscript received Feb. 5, 2014; accepted for publication Feb. 6, 2014; published online Mar. 10, 2014.

1 Introduction

Photopolymerization[1,2] is a widely used method to harden polymers in a controllable manner by illuminating a liquid monomer or an uncured polymer precursor. Originally used in the field of coatings, printing, paints, adhesives, optical fibers, etch resist, or printed circuits,[3–6] it quickly found its way into the biomedical sector where photopolymerizable materials are used for dental implants,[7] cell encapsulation,[8] tissue-replacements,[9,10] drug delivery,[11] implant coatings, bio-glues,[12] and microfluidics.[13] However, when materials are introduced and cross-linked in the body by means of photopolymerization, illumination becomes challenging, since surgical procedures tend to be minimally invasive:[14] large-polymer volumes have to be illuminated with small light-emitting surfaces, for example through the tip of an optical fiber.

Bulk or mass photopolymerization is used for thin and thick films.[15] For uniform illumination of nonscattering polymers, the process of photopolymerization is well understood and mostly modeled using the Beer–Lambert law that describes the exponential decay of the incident light intensity. The extinction coefficient is equal to the absorption coefficient, since scattering is neglected and the photopolymerized surface area is that of the illumination area. Figure 1 illustrates the effect of an additive in the form of scattering particles on photopolymerized volumes. Although the illumination time and incident illumination area are the same for the polymer with and without scattering particles, the polymerized volume varies significantly.

Therefore, a model that takes into account scattering and absorption, light dose, and illumination pattern is required to better predict the photopolymerized volume.

In this article, we investigate photopolymerization of implantable tissue replacements, which are injected through a thin needle and then hardened by illumination with an optical light guide. Based on a statistical Monte Carlo[16,17] approach, a model for photopolymerization is presented. Monte Carlo is a well-known method to model light transport through a scattering medium. It consists of tracking single photon packages and predicting their way throughout a predefined volume based on the media's absorption (μ_a), scattering (μ_s), and anisotropy coefficient (g). Monte Carlo studies have been conducted on a broad selection of tissues, for optical neural stimulation,[18] glucose monitoring,[19] cancer detection,[20] and many others. Bulk-photopolymerization

*Address all correspondence to: Andreas Schmocker, E-mail: andreas.schmocker@epfl.ch

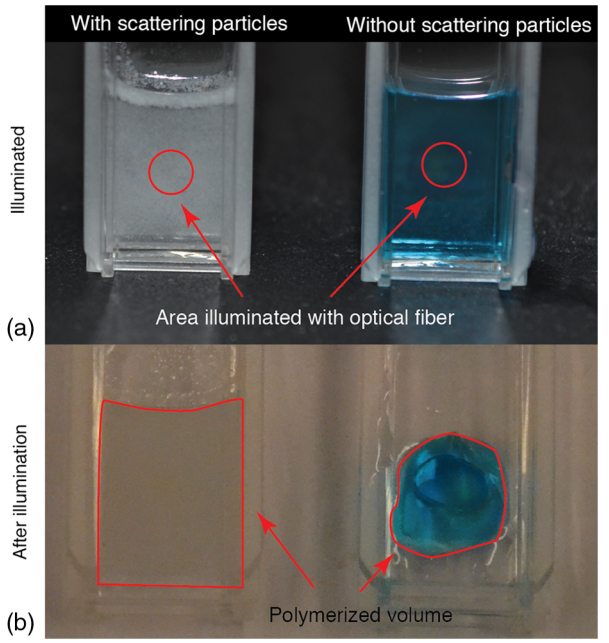

Fig. 1 Poly(ethylene-glycol) dimethacrylate hydrogels. Left: with scattering particles (SP) (intralipids). Right: No SP. The hydrogel without SP has a methylene blue dye to visualize the photopolymerized volume. (a) Samples during illumination. Illumination is performed with the output of a 600-μm-core diameter optical fiber placed 5 mm from the cuvette; (b) after extraction of the unpolymerized liquid. The red lines indicate the polymerized volumes. Light dose and illumination area are the same for both samples.

induced by an incident laser beam has been studied using Monte Carlo[15] or analytical models.[21] However, Monte Carlo modeling of photopolymerization with different absorption, scattering coefficients, and its experimental validation has not been investigated to our knowledge.

This article is organized as follows: the hydrogel precursor composition and fiber-based illumination is introduced in Sec. 2. The experimental method to measure the absorption and scattering coefficients is presented in Sec. 3. Section 4 describes the Monte Carlo simulation model to predict a photopolymerization volume, and Sec. 5 describes its experimental validation. Section 6 models photopolymerization of hydrogels in tissue cavities. An application example of an intervertebral disc replacement is presented. The effect of scattering additives on final polymerization volume is shown. A simple method is proposed to integrate any type of tissue geometry into the simulations.

2 Hydrogel Material and Illumination

We selected a poly(ethylene-glycol) hydrogel because of its commercial availability and interesting biomechanical properties. Due to their elastic strength,[22] swelling ability,[14] and bio-compatibility[23] poly(ethylene-glycol) hydrogel systems are promising for cartilage,[9] tissue replacements,[24] arterial coating,[11] and bio-sensors.[25]

Four different poly(ethylene-glycol)dimethacrylate (PEGDMA) systems were prepared with the following combination of absorption (μ_a) and scattering (μ_s) coefficients: (1) low μ_a and low μ_s, (2) high μ_a and low μ_s, (3) low μ_a and high μ_s, and (4) high μ_a and high μ_s. PEGDMA 6 kDa was synthesized as previously described,[26] the used photoinitiator was Irgacure-2959 (BASF, Ludwigshafen, Germany), and the scattering additives were Intralipids (Fresenius Kabi, Louviers, France). μ_a is adjusted by varying the concentration of the photoinitiator and μ_s is adjusted by adding Intralipids. Phosphate buffer solution was used as the liquid in the hydrogel. Quantities and concentrations are presented in Table 1.

The photoinitiator Irgacure-2959 (1% w/v) absorbs most efficiently between 280 and 320 nm (Fig. 2). Unfortunately, deoxyribonucleic acid nucleotides have their main absorption peaks in this wavelength range[27] and therefore admissible light doses for *in vivo* applications in this range are extremely low.[28] Thus, we opted for a longer wavelength to increase significantly the admissible dose and selected 365 nm, a wavelength where solid-state light-emitting diodes (LEDs) have high brightness and are commercially available. An optical fiber with 600-μm-core diameter, 0.22 numerical aperture (Polymicro Technologies, FVPE60060710/2M), was butt-coupled to a high-power LED chip with emission area of 0.72 mm^2 (Nichia, NCSU033B, Tokushima, Japan). The final fiber optical output power at the fiber tip was 6.5 mW.

3 Determination of Absorption and Scattering Coefficient

In an absorbing and scattering compound, the scattering and absorption coefficients can be measured separately if $\mu_a >> \mu_s, \mu_{ext} = \mu_a + \mu_s \approx \mu_a$ and vice versa for $\mu_a << \mu_s$. In Fig. 3, the setup is presented: the previously described output of the LED fiber-coupled light source is collimated and incident on a 1-mm-thick hydrogel sample sandwiched between two 1-mm-thick glass slides that forms a chamber to confine the liquid and uncrosslinked polymer. The extinction coefficient can be measured throughout the transition from liquid to solid hydrogel. To reduce the optical noise (glass interfaces, local tilts, etc.), the chamber is fixed and can be filled or emptied without moving it. Water is used at a reference before each test. One detector measures the transmitted light and another serves as a reference.

During photopolymerization, the photoinitiator is consumed and a polymer-network forms. Thus, it can be expected that optical properties change during photopolymerization. In the case of the PEGDMA hydrogel, we did not find a significant increase or decrease of the extinction coefficient throughout the photopolymerization reaction for any of the four tested hydrogels. Table 2 shows the measured results for the scattering and absorbing coefficients.

4 Monte Carlo Model for Photopolymerization

Photopolymerization is a multiphysics problem, which includes light transport, bi-phasic (liquid and solid) mass transport (swelling and diffusion), molecular dynamics, and photochemical reactions. The Monte Carlo approach consists of tracking energy

Table 1 Preparation of poly(ethylene glycol) dimethacrylate (PEGDMA) – 6-kDa hydrogel samples.

Sample	PEGDMA 6000 (mg)	Irgacure 2959 (1% w/v) (ml)	Intralipids (10% w/v) (ml)	Phosphate buffer solution (ml)
1. Low μ_a and low μ_s	220	0.22	—	0.659
2. High μ_a and low μ_s	220	0.66	—	0.217
3. Low μ_a and high μ_s	220	0.22	0.1	0.659
4. High μ_a and high μ_s	220	0.66	0.1	0.217

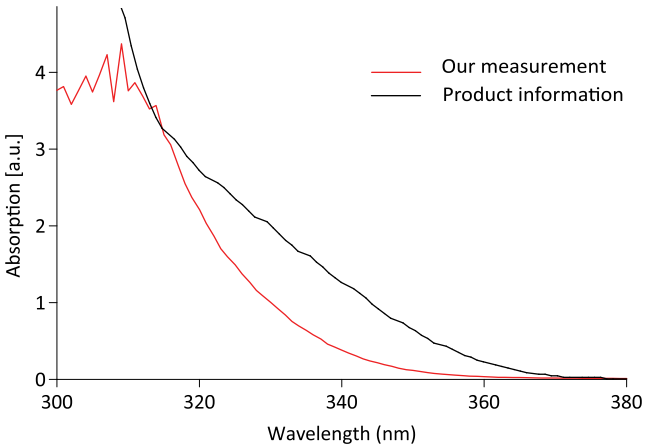

Fig. 2 Absorption curves of the used photoinitiator (Irgacure-2959, 1% w/v). The photosensitizer reacts best around 300 nm, but can also be used at longer, more bio-acceptable wavelengths.

packages through space and thus can account for a maximum of effects. Events like absorption or scattering are characterized statistically. Wang's Monte Carlo model[16,17] (C++ code) was rewritten in MATLAB®. This reduced computational speed considerably, but drastically simplified programming and code validation due to amount of available filter- and spline-functions in MATLAB®. The following assumptions were taken in the model: (1) The initially liquid hydrogel precursor absorbs energy step-wise and at a given threshold, a subvolume (voxel) changes into solid material. (2) The liquid hydrogel precursor and the solid hydrogel are separated by a discrete boundary (different refractive index). As the reaction goes on, this interface changes dynamically. (3) Photons (photon-packages) can be reflected or refracted at this interface and also at the polymer–tissue interface. (4) Scattering and absorption coefficients are dependent on the photon package's position (photon in liquid hydrogel precursor, in solid hydrogel or within tissue). (5) Scattering and absorption coefficients can vary over time (throughout the reaction). Figure 4 shows the modeled intensity distribution of an optical fiber output in hydrogel precursor. One simulation consists of 10^8 photons. After every million-photon package, iso-intensity levels are computed [Fig. 4(b)]. One iso-level is chosen as boundary between solid and liquid hydrogel (e.g., 0.3 or 0.5). This selected iso-level is extracted and thus the volume-growth can be plotted over time [Fig. 4(c)]. The voxel size was chosen to be 10×10 μm.

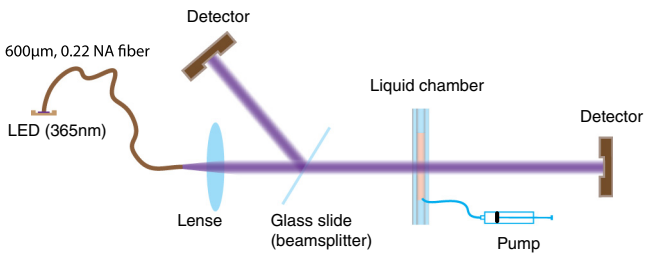

Fig. 3 Transmission setup at 365 nm to measure the extinction coefficient of either a scattering or an absorbing compound. The collimated beam is split into two arms; one is used as reference and the second passes through the sample. The chamber is fixed. Its content can be injected or extracted.

Table 2 Measured scattering and absorbing coefficients at 365 nm (mean and maximal measurement error). These values are used for the simulations (*assumed values for simulations): As extinction-, absorption- and scattering-coefficients linearly depend on molar concentrations of a certain compound, they can be measured individually and then be summed up in a mixed solution.

	Absorption coefficient μ_a (cm^{-1})	Scattering coefficient μ_s (cm^{-1})
1. Low μ_a and low μ_s	0.131 ± 0.003	0.00*
2. High μ_a and low μ_s	0.430 ± 0.004	0.00*
3. Low μ_a and high μ_s	0.131*	6.76 ± 0.48
4. High μ_a and high μ_s	0.430*	6.85 ± 0.62

Due to the statistical nature of Monte Carlo models, solutions have to be averaged over local areas to create proper surfaces between different domains. A median filter (MATLAB®) applied over a neighborhood of 15×15 voxels gives good results as it showed the most similar surfaces compared with experimentally photopolymerized hydrogel samples. The plots in Fig. 4(b) indicate the amount of absorbed energy and need to be correlated to a solid or liquid material state by setting a gel point, the boundary between liquid and solid hydrogel. Brulle et al.[21] proposed, via simulation, to set the gel point at 57% of totally absorbed light energy. Photorheology measurements were performed on the 6-kDa PEGDMA hydrogel and data is shown in Fig. 5(a). Results show that the hydrogel changes from liquid to solid after about 40% of total irradiation energy. Using this information one iso-level [Fig. 4(b)] can be extracted at every time-step to form a growth pattern over time [Fig. 4(c)].

During a simulation run, a photon knows its position, but not the material it is crossing, thus a level-set function φ, attributed to each voxel, is defined:

$$\varphi = \begin{cases} 0 & \text{outside of investigated area} \\ 1 & \text{liquid} \\ 2 & \text{solid} \\ 3 & \text{tissue} \end{cases} . \quad (1)$$

If a photon package crosses the solid–liquid boundary, the stepping algorithm calculates the change in φ, the position where the boundary is crossed, and computes its orientation at the intersection with the photon path [Fig. 5(b)]. Thus, refractions or reflections are calculated dynamically while interfaces change their position. Circularly or linearly polarized light is averaged to compute reflection and refraction probabilities.[17] The algorithm also takes into account time-dependent changes in absorption and scattering coefficients, which can be defined using a desired polynomial function [e.g., $\mu_s(t) = \mu_{s0} + a_1 * t$). Further information on the algorithm is detailed in Ref. 29.

5 Experimental Validation of the Monte Carlo Model

To validate the Monte Carlo model introduced in Sec. 4, four hydrogel samples (Table 1) were placed in a cuvette and illuminated by the previously described, 600-μm-core optical fiber (365 nm). The fiber is touching the liquid polymer

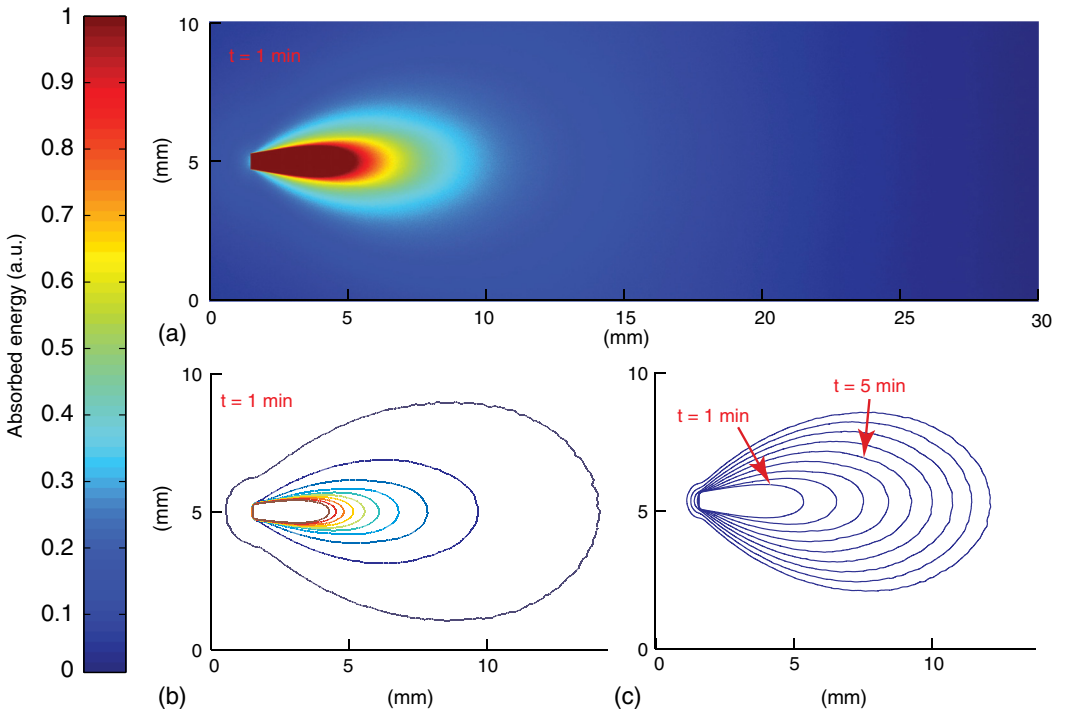

Fig. 4 Monte Carlo simulation of photopolymerized volume. The light source is the output of an optical fiber. (a) Distribution of absorbed energy calculated by the Monte Carlo model. (b) Fitted iso-levels at a given time-step: solid hydrogel in the center and liquid hydrogel precursor outside (c) polymer-volume-growth over time.

[Fig. 6(a)]. The output power at the fiber tip is 6.5 mW. A constant volume of 2 ml of un-cross-linked polymer was injected into the test cuvettes. Samples were photopolymerized during 3, 5, and 10 min. After illumination, the solid polymer was extracted, dried from un-bonded liquid, and weighed. In Figs. 6(b) and 6(c), the volumes and shapes between simulation and experimental results are compared. The experimental volumes and shapes agree very well with the simulated results except for the samples with high absorption and low scattering.

This discrepancy can be explained by the following factors: (1) The Fresnel reflections of the cuvette's side glass walls are taken into account, but not on the cuvette's bottom. (2) The length of the cuvette limits the size (length) of the hydrogel-shape. (3) The simulations do not take into account polymer

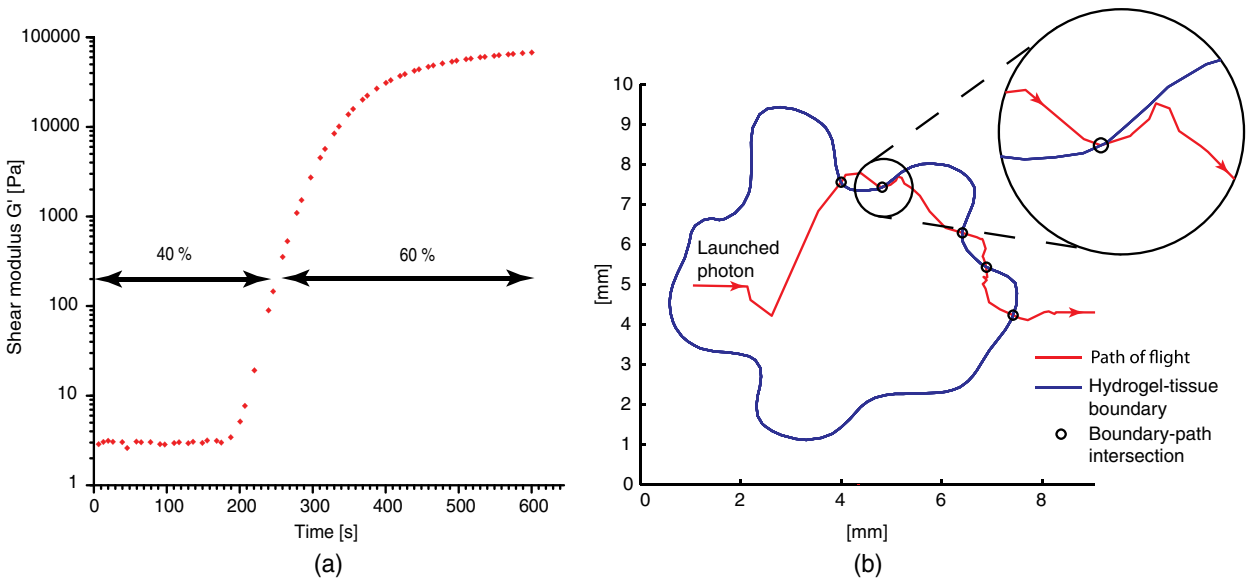

Fig. 5 (a) Photorheology measurement of the poly(ethylene glycol) dimethacrylate (PEGDMA) hydrogel: The gel point (change from liquid to solid) is reached after ~250 s corresponding to 40% of absorbed energy. (b) Interactions of photons with a tissue cavity: The red lines indicate the paths of the tracked photon package.

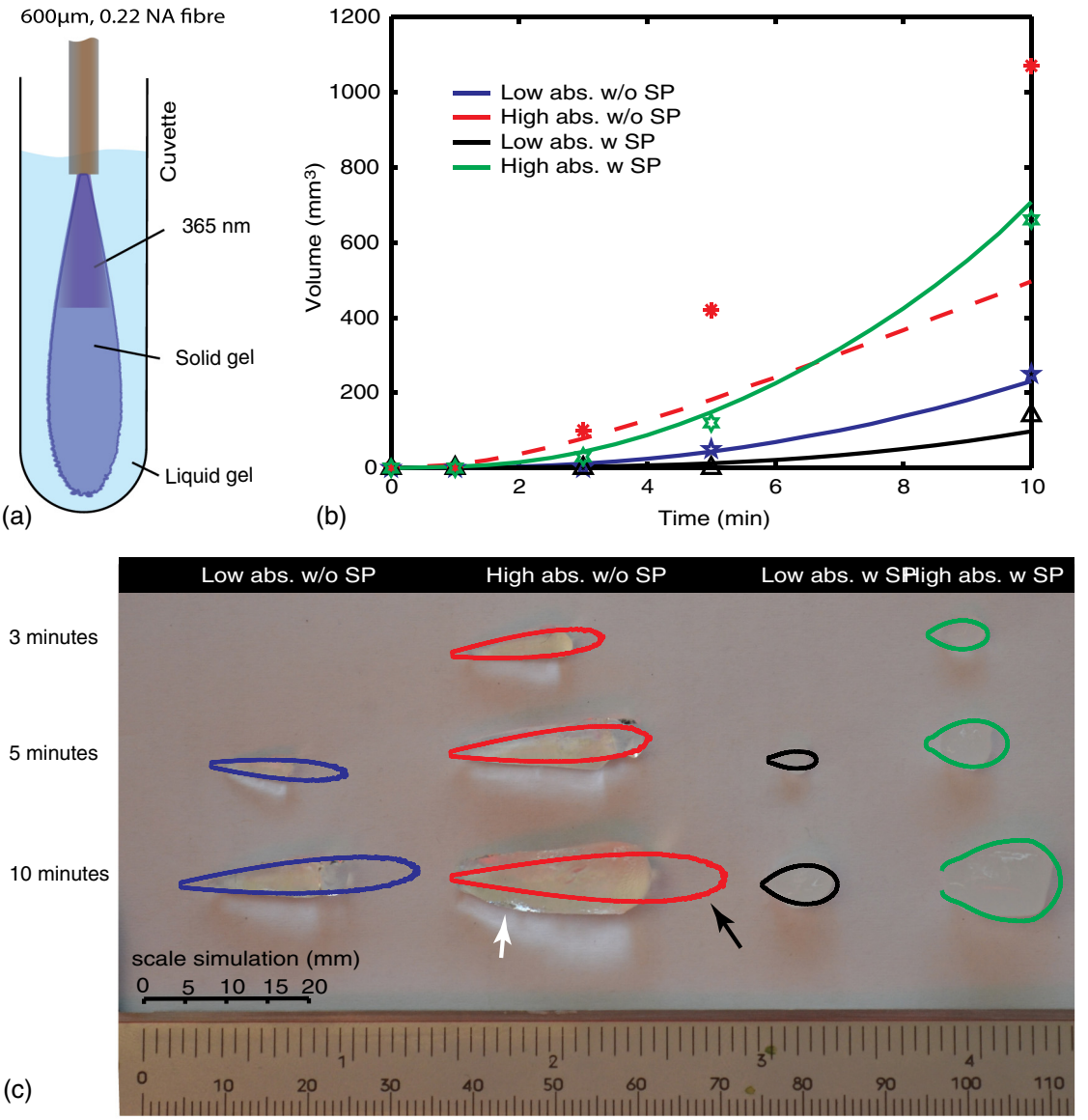

Fig. 6 Four different photopolymerized hydrogel samples (Table 1). (a) Cuvette setup with a fiber immersed into the liquid hydrogel precursor. (b) Volumes of experimentally polymerized samples (stars and triangles) and computed results (colored lines) are compared. (c) Pictures of the shapes of experimentally polymerized and simulated samples (colored contours) after 3, 5, and 10 min of light illumination: The black arrow shows an area where the liquid hydrogel precursor did not solidify due to the size of the cuvette. The white arrow shows an area where polymerization took place due to polymer-diffusion, swelling, and back-reflections.

diffusion, which strongly influences the outcome of photopolymerization.[30,31] As the material diffuses, nucleation is only possible next to already existing solid polymer, thus hydrogel-shapes tend to grow outward of the cone of light (given by the output of the fiber), whereas in the Monte-Carlo simulations the volumes grow within the cone of light.

In the simulations, the energy per photon package is 65 nJ (10^8 photon packages over 16.7 min at 6.5 mW). The amount of photons is 1.2×10^{11} per photon package at 365 nm.

We found that refractions and reflections on the liquid/solid interfaces do not influence photopolymerization outcomes in a significant way. This is because the refractive index between the liquid and solid is approximately $\Delta n = 0.01$ (Ref. 21). We also report that by preilluminating the hydrogel it was possible to photopolymerize volumes up to 3500 mm^3 within 10 min using the previously mentioned 600-μm fiber. The preillumination time was chosen to be equal to the time for which the liquid polymer starts to change its shear modulus (inflexion point in Fig. 5).

6 Modeling and Experimental Application of Photopolymerization in Tissue Cavities

Figure 7 illustrates light scattering and photopolymerization in a tissue cavity. Figure 7(b) shows the autofluorescence of an intervertebral bovine disc cavity injected with a liquid hydrogel monomer and illuminated with 365-nm light from a fiber housed in a rigid needle.

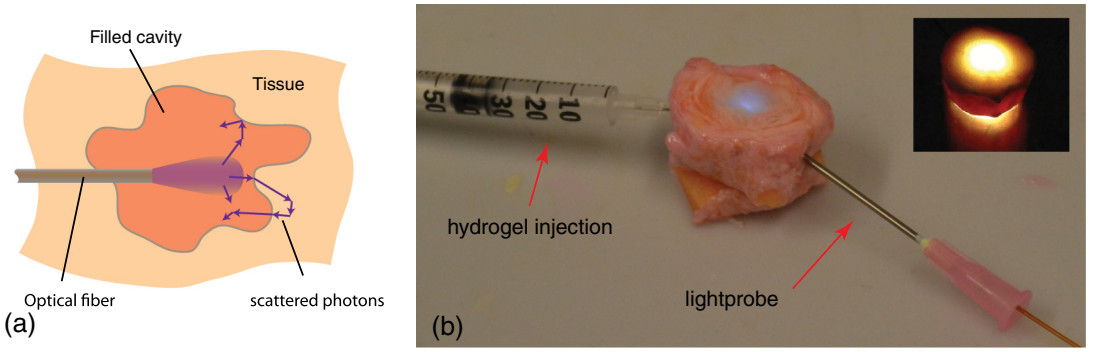

Fig. 7 (a) Schematic: the purple arrows show possible reflections and refractions of back-scattered photons. (b) Autofluorescence of a bovine intervertebral disc tissue cavity (Ref. 32) filled with a PEGDMA-hydrogel and illuminated with a light-probe consisting out of an 18-gauge needle and a 600-μm fiber.

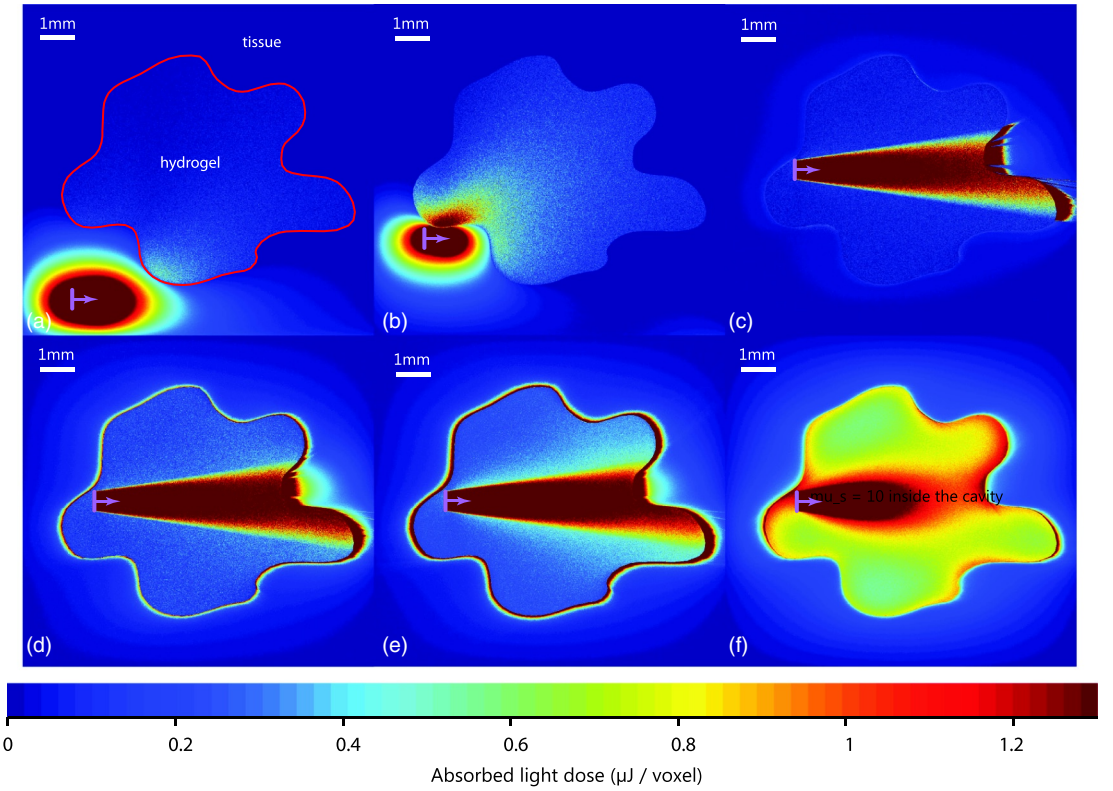

Fig. 8 Photopolymerization of a hydrogel within a tissue cavity: (a) the hydrogel precursor ($\mu_a = 0.43$ cm^{-1}, variable μ_s) is injected into the cavity. The surrounding tissue is modeled with an absorption coefficient of $\mu_a = 0.33$ cm^{-1} and scattering coefficient $\mu_s = 210$ cm^{-1}. An optical fiber (violet arrow) is introduced into/next to the cavity (NA = 0.22, diameter 600 μm), the color-scale indicates the amount of absorbed energy per voxel. The hydrogel precursor requires a minimal irradiance of 0.52 μJ per voxel corresponding to a fluence of 520 mJ/cm^2 for photopolymerization. (a) The probe is placed several millimeters away from the cavity, (b) the probe is located next to the cavity wall, (c) the probe is in the cavity, no scattering additives are present in the gel ($\mu_s = 0.000$ cm^{-1}), (d) low amount of SP ($\mu_s = 0.1$ cm^{-1}), (e) medium amount of SP ($\mu_s = 1$ cm^{-1}), and (f) high amount of SP ($\mu_s = 10$ cm^{-1}).

The surrounding tissue absorbs light, but it can also reflect and scatter it, which directly alters the local irradiance and thus photopolymerization [Fig. 7(b)]. Photopolymerization, light source, and interactions of tissue/polymer interfaces with photons were modeled with the Monte Carlo model presented in Secs. 4 and 5. The energy absorbed (light dose) by the hydrogel is shown in Fig. 8. The tissue cavity was designed arbitrarily using a drawing software (Illustrator).

The position of the fiber-tip is important [Figs. 8(a)–8(c)]. Missing the cavity by a distance of <500 μm [Fig. 8(b)] leads to no significant light dose in the cavity. In Fig. 8(c), the polymerized volume is 38.1 mm^2, whereas in Fig. 8(b) it is only 2.2 mm^2 and in Fig. 8(a) it is 0 mm^2. We observe in Fig. 8(c) that even if the probe is placed at the right position the low-scattering coefficient and the high-absorption coefficient does not lead to a complete polymerization of the cavity volume. By adding scattering particles, the scattering coefficient rises [Figs. 8(c)–8(f)] and the amount of photopolymerized hydrogel can be increased by a factor 4 to 152.4 mm^2 [Fig. 8(f)], where the cavity is completely filled with solid polymer. There is an optimal amount of

scattering particles which can be added to the gel. If this amount is too low [Fig. 8(e)] light is scattered weakly and most of it is absorbed at the cavity edge. We find that a scattering coefficient $\mu_s = 10\ \mathrm{cm}^{-1}$ leads to an adequate level of scattering that provides a uniformly absorbed-light dose in the cavity. If the concentration of scattering particles increases further, the light is not able to reach the edges of the cavity anymore.

7 Conclusion

A simple and robust photopolymerization Monte Carlo model is presented and applied to the case, where the dimension of the light source is much smaller than the volume of the photopolymerizable hydrogel. The model was validated and compared with experimental results by using a PEGDMA hydrogel. Good agreement between predicted and actual polymer volumes and shapes was found. Reflection and refraction effects at solid–liquid interfaces did not impact the shape or volume of photopolymerized material. Our *in vitro* experiments show that uniform spherical volumes up to 700 mm^3 can be photopolymerized in 10 min using intralipids, and that by preilluminating a hydrogel precursor, a volume of up to 3500 mm^3 can be reached. Simulations and photopolymerization experiments inside a cavity filled with a hydrogel provide insights into the polymer–light–tissue interactions. We observed that the probe position is crucial and that a certain amount of scattering particles increases the polymerized volume by a factor of 4. Furthermore, it is conceivable that a gradient of scattering particles in the hydrogel is used to tailor the polymerization rates of certain areas and hence their mechanical properties. Thus, by means of simulations and *in situ* experiments, this article shows the potential for injecting and hardening photopolymerizable, optically scattering hydrogel implants through a small-diameter fiber thus paving the way for minimal invasively implanted tissue replacements or scaffolds.

Acknowledgments

The authors thank Dr. Georges Wagnières for his advice on the Monte Carlo model. Funding for this research was provided by the Swiss National Fund (#10024003165465).

References

1. J. S. Owens, "US patent: Photopolymerization methode," US patent US2344785 (1944).
2. G. Oster, "Dye-sensitized photopolymerization," *Nature* **173**(4398), 300–301 (1954).
3. G. Odian, *Principles of Polymerization, Principles of Polymerization*, 4th ed., pp. 198–349, John Wiley & sons, Inc. (2004).
4. M. Sangermano et al., "One-pot photoinduced synthesis of conductive polythiophene-epoxy network films," *Polymer (Guildf)* **54**(8), 2077–2080 (2013).
5. K. S. Anseth, C. M. Wang, and C. N. Bowman, "Kinetic evidence of reaction diffusion during the polymerization of multi(meth)acrylate monomers," *Macromolecules* **27**(3), 650–655 (1994).
6. H. Zhang et al., "In situ solvothermal synthesis and characterization of transparent epoxy/TiO2 nanocomposites," *J. Appl. Polym. Sci.* **125**(2), 1152–1160 (2012).
7. K. Ikemura et al., "UV-VIS spectra and photoinitiation behaviors of acylphosphine oxide and bisacylphosphine oxide derivatives in unfilled, light-cured dental resins," *Dent. Mater. J.* **27**(6), 765–774 (2008).
8. M. P. Lutolf and J. A. Hubbell, "Synthetic biomaterials as instructive extracellular microenvironments for morphogenesis in tissue engineering," *Nat. Biotechnol.* **23**(1), 47–55 (2005).
9. S. J. Bryant, G. D. Nicodemus, and I. Villanueva, "Designing 3D photopolymer hydrogels to regulate biomechanical cues and tissue growth for cartilage tissue engineering," *Pharm. Res.* **25**(10), 2379–2386 (2008).
10. D.-A. Wang et al., "Multifunctional chondroitin sulphate for cartilage tissue-biomaterial integration," *Nat. Mater.* **6**(5), 385–392 (2007).
11. Y. An and J. A. Hubbell, "Intraarterial protein delivery via intimally-adherent bilayer hydrogels," *J. Control. Release* **64**(1–3), 205–215 (2000).
12. J. Vernengo et al., "Synthesis and characterization of injectable bioadhesive hydrogels for nucleus pulposus replacement and repair of the damaged intervertebral disc," *J. Biomed. Mater. Res. B. Appl. Biomater.* **93**(2), 309–317 (2010).
13. H. M. Simms et al., "In situ fabrication of macroporous polymer networks within microfluidic devices by living radical photopolymerization and leaching," *Lab Chip* **5**(2), 151–157 (2005).
14. K. T. Nguyen and J. L. West, "Photopolymerizable hydrogels for tissue engineering applications," *Biomaterials* **23**(22), 4307–4314 (2002).
15. K. Yamaguchi and T. Nakamoto, "Micro fabrication by UV laser photopolymerization," *Mem. Sch. Eng. Nagoya Univ.* **50**(1/2), 33–82 (1998).
16. L. Wang, S. L. Jacques, and L. Zheng, "MCML—Monte Carlo modeling of light transport in multi-layered tissues," *Comput. Methods Programs Biomed.* **47**(2), 131–146 (1995).
17. L. Wang and S. Jacques, "Monte Carlo modeling of light transport in multi-layered tissues in standard C," Ph.D. Thesis, University of Texas, MD Anderson (1992).
18. A. C. Thompson et al., "Modeling of light absorption in tissue during infrared neural stimulation," *J. Biomed. Opt.* **17**(7), 075002 (2012).
19. X. Wang, G. Yao, and L. V. Wang, "Monte Carlo model and single-scattering approximation of the propagation of polarized light in turbid media containing glucose," *Appl. Opt.* **41**(4), 792–801 (2002).
20. K. Steenland and S. Greenland, "Monte Carlo sensitivity analysis and Bayesian analysis of smoking as an unmeasured confounder in a study of silica and lung cancer," *Am. J. Epidemiol.* **160**(4), 384–392 (2004).
21. Y. Brulle et al., "Industrial photochemistry XXI. Chemical, transport and refractive index effects in space-resolved laser photopolymerization," *J. Photochem. Photobiol. A Chem.* **83**(1), 29–37 (1994).
22. S. J. Bryant et al., "Crosslinking density influences the morphology of chondrocytes photoencapsulated in PEG hydrogels during the application of compressive strain," *J. Orthop. Res.* **22**(5), 1143–1149 (2004).
23. B. D. Fairbanks et al., "Photoinitiated polymerization of PEG-diacrylate with lithium phenyl-2,4,6-trimethylbenzoylphosphinate: polymerization rate and cytocompatibility," *Biomaterials* **30**(35), 6702–6707 (2009).
24. C. Eyholzer et al., "Biocomposite hydrogels with carboxymethylated, nanofibrillated cellulose powder for replacement of the nucleus pulposus," *Biomacromolecules* **12**(5), 1419–1427 (2011).
25. M. Heuberger, T. Drobek, and N. D. Spencer, "Interaction forces and morphology of a protein-resistant poly(ethylene glycol) layer," *Biophys. J.* **88**(1), 495–504 (2005).
26. S. Lin-Gibson et al., "Synthesis and characterization of PEG dimethacrylates and their hydrogels," *Biomacromolecules* **5**(4), 1280–1287 (1994).
27. Y. Hiraku et al., "Photosensitized DNA damage and its protection via a novel mechanism," *Photochem. Photobiol.* **83**(1), 205–212 (2007).
28. N. B. O. S. Counselors, "Report on carcinogens background document for ultraviolet (UV) radiation and UVA, and UVB, and UVC," Report on Carcinogens Background Document for Broad Spectrum Ultraviolet (UV) Radiation and UVA, and UVB, and UVC (2000).
29. A. Schmocker et al., "Multi-scale modeling of photopolymerization for medical hydrogel-implant design," *Proc. SPIE* **8592**, 85921D (2013).
30. H. J. Naghash, O. Okay, and Y. Yağci, "Gel formation by chain-crosslinking photopolymerization of methyl methacrylate and ethylene glycol dimethacrylate," *Polymer (Guildf)* **38**(5), 1187–1196 (1997).
31. V. V. Krongauz and R. M. Yohannan, "Photopolymerization kinetics and monomer diffusion in polymer matrix," *Polymer (Guildf)* **31**(6), 1130–1136 (1990).
32. S. C. W. Chan et al., "Papain-induced in vitro disc degeneration model for the study of injectable nucleus pulposus therapy," *Spine J.* **13**(3), 273–283 (2013).

Andreas Schmocker is a PhD student at the Federal Institute of Technology in Lausanne. He received his BS and MS degrees in mechanical-, bio-mechanical engineering and management of technology from the same university in 2007 and 2009, respectively. His current research interests include medical- and photonic-device development. He is a winner of a McKinsey award and a member of SPIE, OSA, and SSBE.

Biographies of the other authors are not available.